An experimental study of the instability of the laminar Ekman boundary layer

By ALAN J. FALLER

Woods Hole Oceanographic Institution, Woods Hole, Mass.

(Received 14 May 1962 and in revised form 3 October 1962)

This study concerns the stability of the steady laminar boundary-layer flow of a homogeneous fluid which occurs in a rotating system when the relative flow is slow compared to the basic speed of rotation. Such a flow is called an Ekman boundary-layer flow after V. W. Ekman who considered the theory of such flows with application to the wind-induced drift of the surface waters of the ocean.

Ekman flow was produced in a large cylindrical rotating tank by withdrawing water from the centre and introducing it at the rim. This created a steady-state symmetrical vortex in which the flow from the rim to the centre took place entirely in the shallow viscous boundary layer at the bottom. This boundary-layer flow became unstable above the critical Reynolds number $Re_c = vD/\nu = 125 \pm 5$, where v is the tangential speed of flow, $D = (\nu/\Omega)^{\frac{1}{2}}$ is the characteristic depth of the boundary layer, ν is the kinematic viscosity, and Ω is the basic speed of rotation. The initial instability was similar to that which occurs in the boundary layer on a rotating disk, having a banded form with a characteristic angle to the basic flow and with the band spacing proportional to the depth of the boundary layer.

1. Introduction

Stability criteria for laminar viscous flows have been a major goal of studies in theoretical fluid dynamics for many years. But because of inherent complexities involved in the solution of the hydrodynamic perturbation equations very few exact solutions for stability criteria have been obtained (for an excellent survey see Lin 1955). These have been confined for the most part to physical situations which may be described as having two-dimensional flow, that is, examples in which the velocity vector and the shear vector at every point lie in the same plane. However, many régimes in which the question of stability is an important one are not two-dimensional, but the additional complexities associated with the angular variation of the flow have rendered the exact mathematical analysis intractable.

An example which has received considerable attention is the flow induced by a rotating circular disk in still air. In an experimental study Gregory, Stuart & Walker (1955) (hereafter referred to as GSW) confirmed the velocity profiles deduced theoretically and determined a critical Reynolds number for the onset of instability. Furthermore, Stuart's mathematical analysis provided physical insight into the nature of the instability and successfully explained certain features of the evolved flow. The instability which was observed had the form of

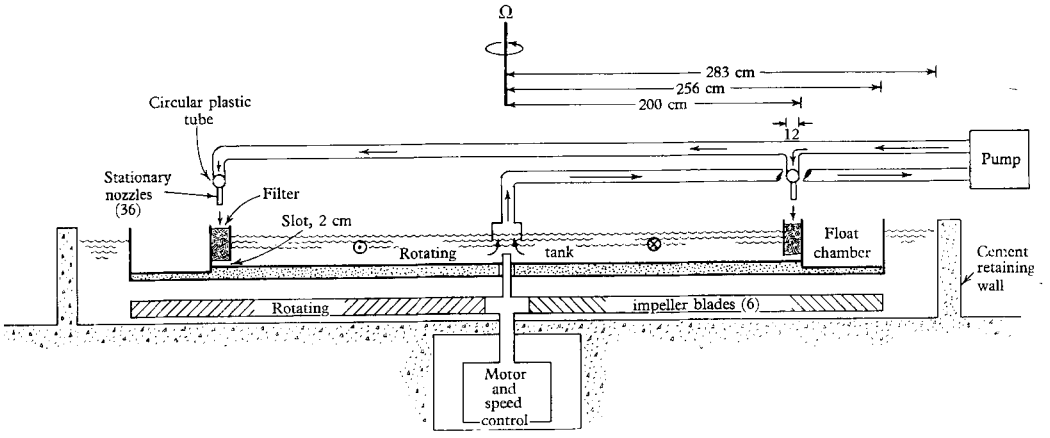

FIGURE 1. Schematic diagram of the rotating tank and mechanism.

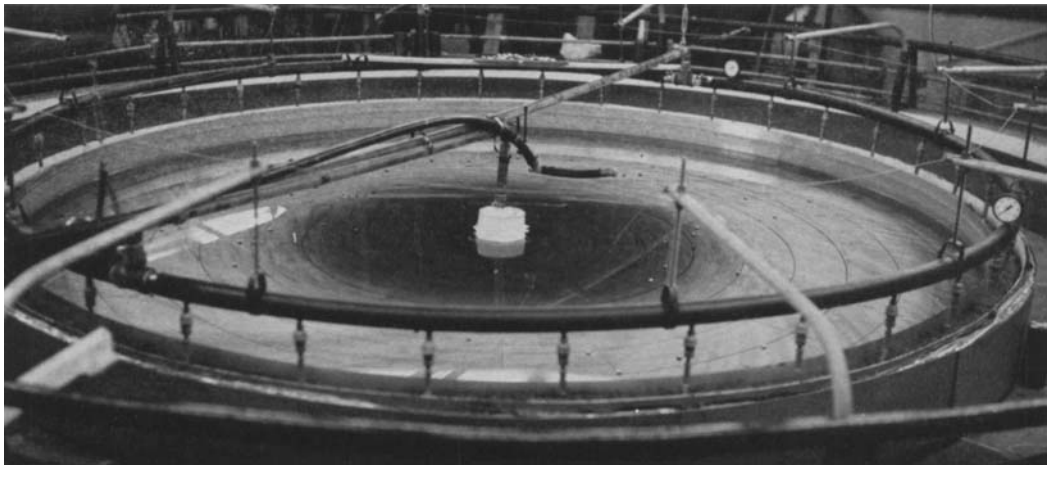

FIGURE 2. Photograph of the apparatus in operation without the central core.

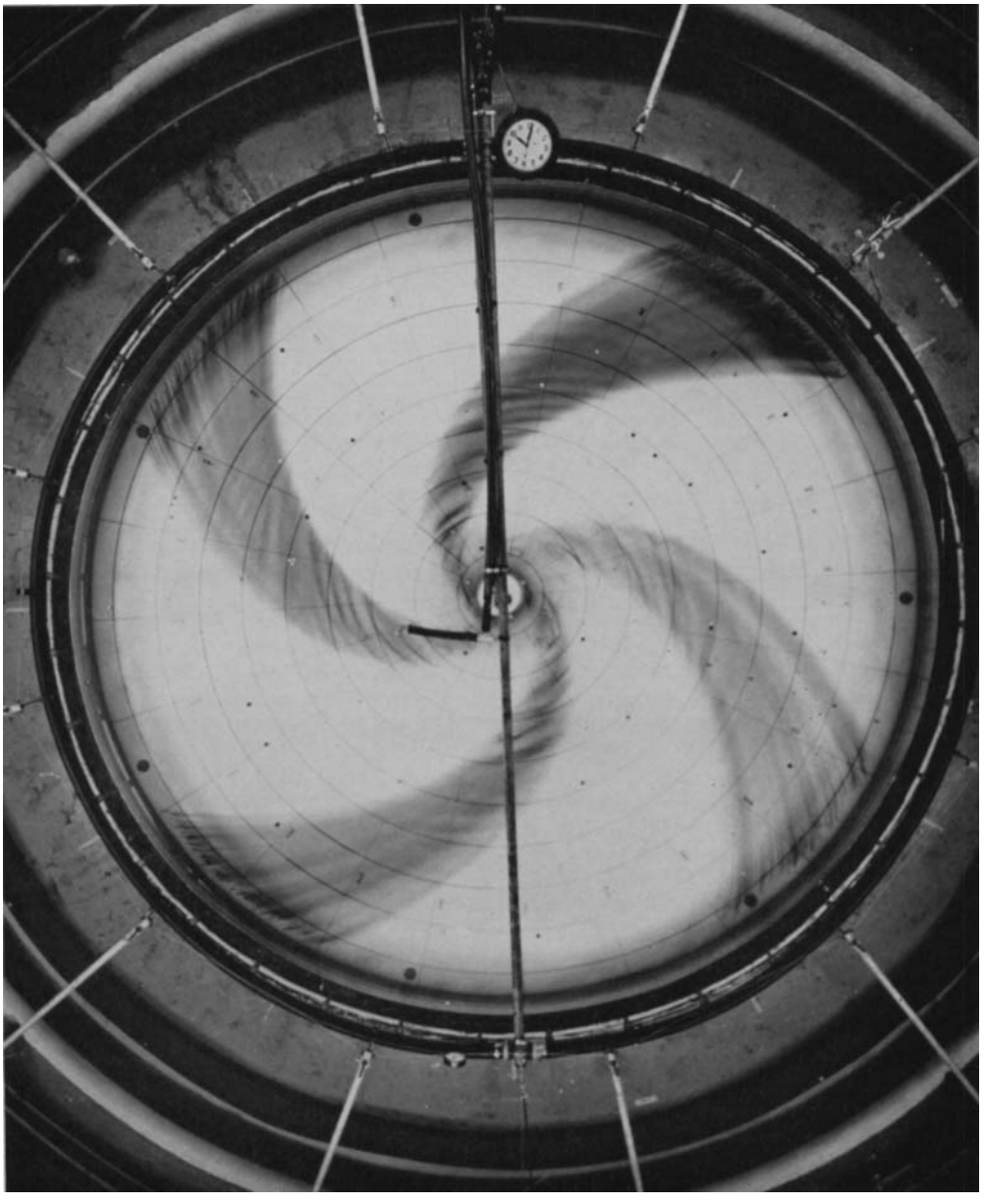

FIGURE 3. The rotating tank as seen from above with an example of the pattern of instability of the Ekman boundary layer. The major spiral arms with the crossing angle of approximately 45° are caused by the selective introduction of dye in 4 sectors of the tank. They demonstrate the inflow at the bottom of the boundary layer. The spiral bands formed by the instability of the laminar boundary layer begin in this case at approximately $r = 0{\cdot}60$.

(*a*)

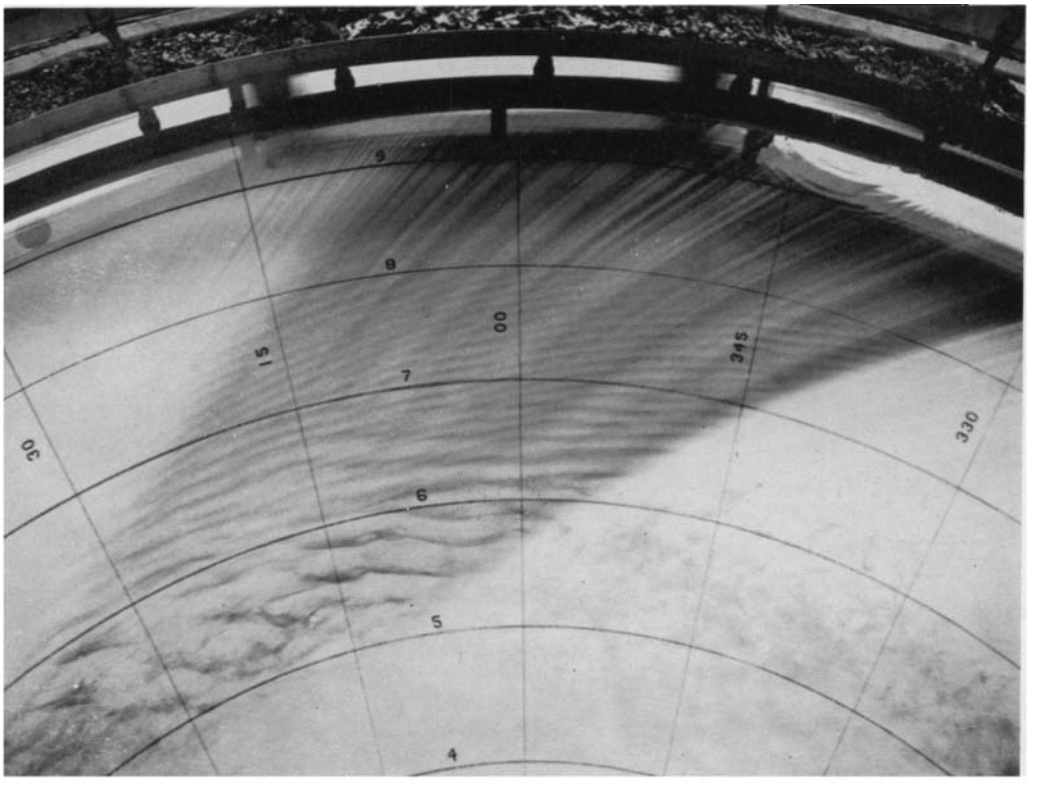

(*b*)

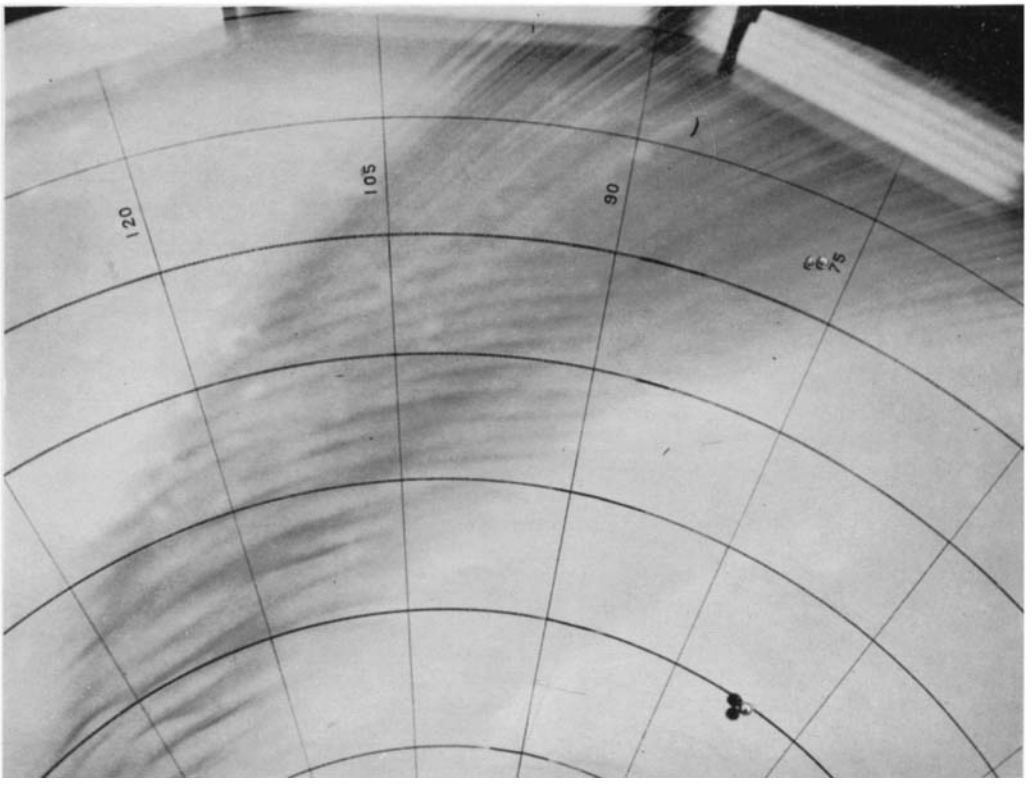

For legend see p. 561.

(c)

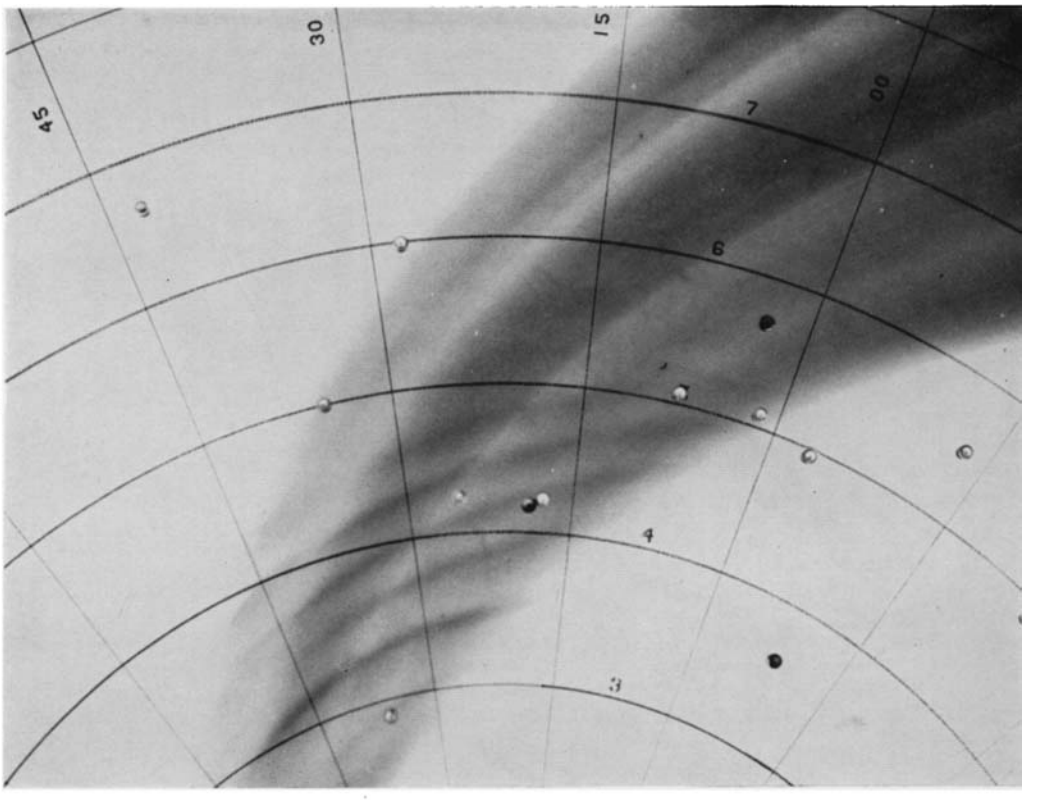

(d)

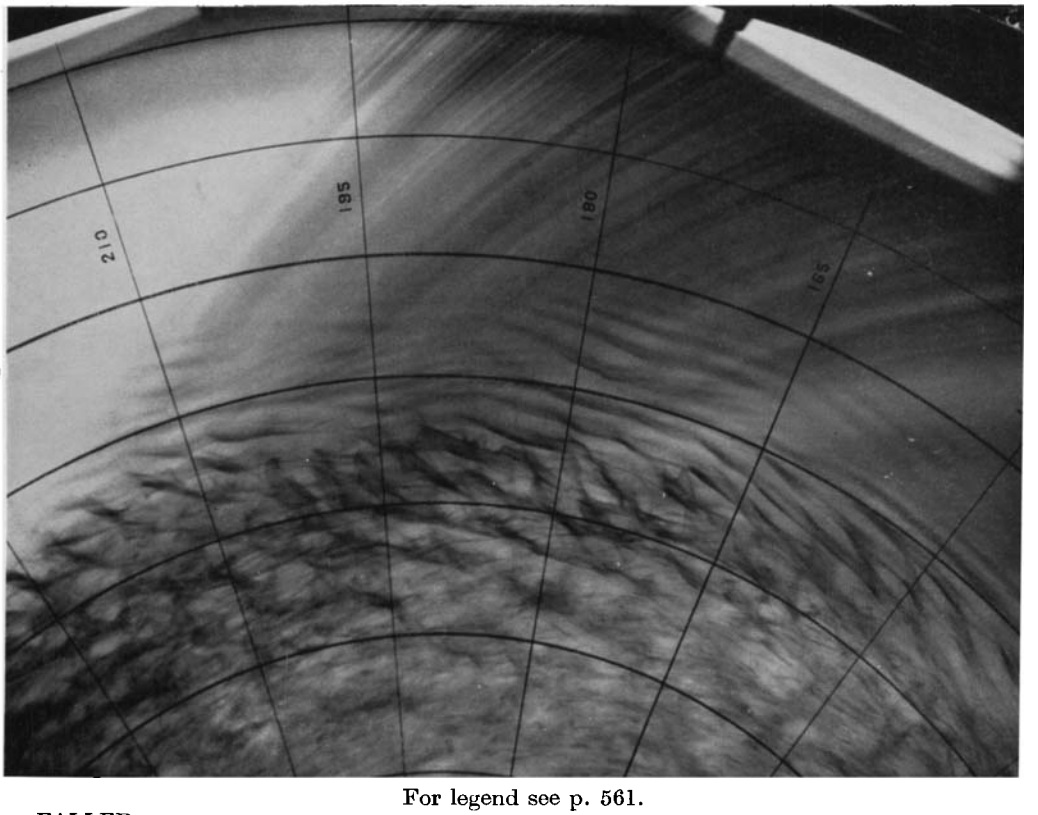

For legend see p. 561.

stationary roll vortices with a spacing related to the depth of the boundary layer and oriented at a small characteristic angle with respect to the tangential direction on the disk. Gregory & Walker (1960) extended the study of instability to a rotating disk with suction.

An important feature of those particular three-dimensional circulations from the viewpoint of theoretical fluid dynamics is that the basic flow has been determined from exact numerical solutions to the Navier–Stokes equations of motion. These have been obtained by von Kármán (1921) and Cochran (1934) for the rotating disk and for the disk with suction by Stuart (1954) and Fettis (1955). Mathematical proof of the existence of the flow described by Fettis has been given by Howard (1961) for a certain range of the suction parameter.

The experimental study reported here is concerned with the stability of the laminar Ekman (1905) boundary layer which has an exact *analytical* solution. Laminar Ekman flow was obtained by the generation of a vortex in a large rotating tank, the vortex being produced by withdrawing water from the centre of the tank and by re-supplying it at the rim (see figures 1 and 2, plate 1). After transient motions have subsided the flow consists essentially of a tangential circulation throughout the main body of the fluid whose speed relative to the rotating apparatus is slow and inversely proportional to the radius, and a boundary-layer flow near the bottom. This latter flow accomplishes the entire radial transport.

Boundary-layer instability of the same general nature as that reported by GSW has been found (see figure 3, plate 2 and figure 4, plates 3, 4) but with the following major differences in the experimental results: (1) a significantly different value of the critical Reynolds number was found, and (2) the observed perturbations were of a different wavelength and generally were not stationary.

Other papers have been published recently on the theoretical possibility (Stern 1960) and on the experimental manifestations (Arons, Ingersol & Green 1961) of instability of laminar Ekman flow, but these papers were concerned with forms of instability of a basically different nature from that which is discussed here. For example, the perturbation described in the latter paper extended through the entire depth of fluid and occurred at relative speeds of flow lower than the critical values found here by more than an order of magnitude. Specifically, this work describes an instability which is entirely a boundary-layer phenomenon, whereas the above papers were concerned with examples in which the instability involved the interaction of the boundary-layer flow with the interior circulation.

This work was initiated as part of a study of certain boundary-layer flows

---

EXPLANATION OF PLATES 3 AND 4

FIGURE 4. Examples of patterns of dye in the boundary layer caused by the instability.

		Ω (sec^{-1})	S (cm^3 sec^{-1})
Plate 3	(*a*) 7. iv. 60, VII	0·390	840
	(*b*) 14. iv. 60, V,	0·094	650
Plate 4	(*c*) 7. iv. 60, I	0·027	568
	(*d*) 7. iv. 60, IX	0·393	588

Note the increased spacing of the bands from (*a*) to (*c*) because of the decrease of Ω, and the decrease of the radius of instability because of the decrease of S.

in rotating systems with intended application to experimental model studies of geophysical fluid circulations. Boundary-layer velocity profiles which approximate Ekman flow occur in the atmospheric boundary layer to a height of perhaps 1000 m, and in the wind-driven surface layer of the ocean to a depth of the order of 50 m. However, possible analogies with geophysical flows are not considered in detail here because the oceanic and atmospheric examples always involve turbulence due to rough boundary surfaces, thermal instability, or complicated time and space variations of the energy sources. In contrast these experiments are concerned with the steady laminar flow of a uniform fluid.

Some mention should be made of other relevant studies of boundary-layer flows. Stewartson (1953) found an expansion solution (by a method similar to that developed here) for a disk rotating at a small differential speed with respect to a fluid in uniform rotation at infinity. Haurwitz (1935) previously had found an analytical solution for arbitrary values of the angular rotation of the fluid and that of the disk, although he had to neglect vertical motion due to convergence in the boundary layer. More recently, Rogers & Lance (1960) have obtained complete numerical solutions over a wide range of conditions with the fluid at infinity in solid rotation or at rest. The flow considered here differs from those discussed above in that mass continuity in this case specifies no net convergence in the boundary layer. The solutions of Rogers & Lance or of Stewartson are not directly applicable because of the different variation of the basic flow with radius and the consequent flux of mass into or out of the boundary layer when the fluid at infinity is in solid rotation.

2. Experimental apparatus and observational techniques

Figure 1 (plate 1) is a schematic diagram and figure 2 (plate 1) is a photograph of the rotating tank which was built by von Arx (1955) for studies of the wind-driven ocean circulation. The support and driving mechanism, by flotation and impeller blades, assured smooth rotation and stable speeds, and the original design was altered for this study only by installation of a central shaft with a flexible bearing to prevent lateral oscillations of the tank at the higher rotation speeds. The inside floor of the rotating tank was smoothed and levelled with a poured thermosetting polyester resin. The pumping system withdrew water from the centre of the tank and distributed it uniformly around the rim by means of 36 equally spaced stationary nozzles. The rotation of the tank served to smooth the distribution of water, and a filter of rubberized-hair packing material and a set of baffles brought the water to the basic rotation speed before it flowed into the boundary layer through the 2 cm high gap at the bottom of the outer rim. In the first set of experiments a central core with a rim of radius 54 cm and with a 2 cm gap at the bottom was used, and part of the data (up to 29. iii. 60, VIII in table 1) was obtained with this inner rim. There was no noticeable effect of this vertical boundary beyond a radius of 60 cm but it was removed for later experiments to permit observations at smaller radii.

The basic controlled variables of the experiments were the flow rate S, determined from a calibrated water meter read at 1 min intervals; the basic rotation

Experiment		Ω (sec^{-1})	S ($cm^3\,sec^{-1}$)	$\nu \times 10^2$ ($cm^2\,sec^{-1}$)	H (cm)	r_c	Re_c	Ro_c	D (cm)	l_c (cm)	L	α (deg.)
15. iii. 60	I	0·523	526	1·20	12·5	0·49	142	0·110	0·152	1·54	10·9	10·0
	II	0·240	516	1·20	12·5	0·49	140	0·160	0·224	2·27	11·5	10·5
	V	0·249	535	1·14	8	0·54	139	0·138	0·214	1·98	10·5	13·0
29. iii. 60	II	0·263	715	1·16	20	0·70	140	0·105	0·210	2·27	11·3	10·0
	III	0·263	562	1·15	20	0·57	137	0·126	0·209	2·04	10·8	14·0
	IV	0·266	456	1·14	20	0·45	142	0·163	0·207	1·97	10·7	15·0
	VII	0·105	568	1·10	20	0·58	142	0·198	0·324	2·97	10·1	16·3
	VIII	0·105	456	1·10	20	0·47	141	0·242	0·324	3·04	11·6	15·5
7. iv. 60	I	0·027	568	1·11	25	0·50	163	0·520	0·639	5·58	10·4	—
	IV	0·529	689	1·08	25	0·75	136	0·065	0·143	1·78	12·7	—
	IX	0·393	588	1·07	25	0·64	138	0·089	0·165	—	—	—
12. iv. 60	I	0·237	474	1·19	20	0·44	144	0·184	0·224	2·13	11·6	10·0
	II	0·236	618	1·17	20	0·59	142	0·135	0·223	2·16	10·4	—
	V	0·100	457	1·13	20	0·42	154	0·307	0·336	2·84	9·6	15·0
	VI	0·099	627	1·12	20	0·60	149	0·208	0·336	3·58	11·6	12·5
	IX	0·038	440	1·08	20	0·40	162	0·537	0·530	5·46	11·8	—
14. iv. 60	I	0·238	505	1·17	25	0·50	137	0·153	0·222	2·08	10·9	12·5
	II	0·236	710	1·16	25	0·70	139	0·110	0·222	2·25	11·1	13·0
	IV	0·095	505	1·11	25	0·50	145	0·248	0·342	3·24	10·1	15·0
15. iv. 60	I	0·233	622	1·03	25	0·67	144	0·112	0·210	2·14	11·0	13·0
22. iv. 60	I	0·234	421	1·11	20	0·40	151	0·206	0·218	2·06	10·9	—
	II	0·234	580	1·10	20	0·59	142	0·131	0·217	2·06	10·2	11·0

TABLE 1

rate of the tank, Ω; the kinematic viscosity, ν, determined from the temperature and the tabulations of Dorsey (1940); and the total depth of fluid, H. The ranges of these variables may be seen in table 1, and the values of each independent variable are believed to have departed from the true values with a standard deviation of error not exceeding 1 %. The primary dependent variables considered in this study are: the tangential speed of flow v as a function of radius r, the observed critical radii of transition from laminar to wave motions r_c, the wave lengths l_c and the angles α of the observed unstable waves after the transition from laminar flow, and the relative speeds of motion of the bands.

The tangential flow was recorded by a sequence of photographs which showed the positions of tracers floating near the surface of the water. Small light bulbs $2\frac{1}{2}$ cm long were used as floating tracers since they were well imbedded into the fluid and moved quite independently of wind stress or surface films. A reference grid was painted onto the bottom of the tank and the necessary corrections for the positions of the tracers including parallax and refraction at the sloping air–water interface have been applied. The character of the circulation in the boundary layer was made evident by the introduction of crystals of potassium-permanganate dye near the outer rim (see figure 3, plate 2). *Streaks* from the dye crystals extended inward in nearly-equiangular spirals with angles very close to the 45 degrees predicted by the boundary-layer theory of the flow immediately above the boundary.† The spiral *bands* of dye (and alternate clear bands) which formed as a result of the instability of the boundary-layer flow can be seen in figure 3 (plate 2) and figure 4 (plates 3, 4). These bands are interpreted as regions in the bottom of the boundary layer where the thin layer of dyed fluid became deeper (or shallower) because of the slower (or faster) speeds of flow associated with the superposition of unstable perturbations upon the basic boundary-layer flow.

3. Theory of the basic circulation

A simplified analysis of the circulation to be expected for very slow flow was presented in an earlier paper (Faller 1960). However, in this study it was necessary to use somewhat higher speeds of flow to achieve instability, and consequently neglect of the non-linear inertial terms in the equations of motion is not justified. To take into account the non-linearities an iteration solution based upon an expansion in powers of a Rossby number was obtained, the Rossby number being a small parameter which measures the ratio of characteristic non-linear terms to the Coriolis acceleration. With the following transformations the Navier–Stokes equations may be rewritten in a suitable non-dimensional form:

$$z' = zD, \quad r' = rR,$$
$$u = cU/r, \quad v = cV/r, \quad w = DcW/R, \quad c = S/\pi RD,$$
$$P_r = rp_r^*/2\Omega cD, \quad P_z = p_z^*/2\Omega cD, \quad p^* = (p/\rho - \tfrac{1}{2}\Omega^2 r'^2 + gz'),$$
$$Ro = c/2\Omega r^2 R, \quad Ek = (\nu/\Omega H^2)^{\frac{1}{2}} = D/H, \quad T = \Omega^2 R^4/\nu^2 = R^4/D^4.$$

† Detailed measurements of the angles of the dye streaks have shown a variation of angle with radius as the dye moves inward and diffuses upward. This variation in angle has been found (Faller 1962) to be in good agreement with the theoretical boundary-layer flow where the height of the dye was estimated from a simple diffusion theory.

The notation is as follows:

r', θ, z'	right-handed polar co-ordinates
r, z	non-dimensional radial and vertical co-ordinates
u, v, w, p	dimensional velocity components and pressure, the dependent variables.
U, V, W, P	the non-dimensional dependent variables
ρ, ν, g	density, kinematic viscosity, and acceleration of gravity
H, R	depth and radius of the fluid cylinder
Ω, S	angular rotation speed and the forced volume-rate of flow
D	a characteristic horizontal boundary-layer depth
c	a characteristic speed of flow
Ro	the Rossby number
Ek	the Ekman number
T	the Taylor number

The equations of motion and of continuity for the steady symmetrical flow of a homogeneous fluid may then be written

$$Ro(UrU_r - U^2 - V^2 + r^2 WU_z) - \underline{V = P_r + U_{zz}} + T^{-\frac{1}{2}}(U_{rr} - U_r/r), \tag{1}$$

$$Ro(UrV_r + r^2 WV_z) + \underline{U = V_{zz}} + T^{-\frac{1}{2}}(V_{rr} - V_r/r), \tag{2}$$

$$Ro(UrW_r + r^2 WW_z) = T^{\frac{1}{2}}P_z + W_{zz} + T^{-\frac{1}{2}}(W_{rr} + W_r/r), \tag{3}$$

$$U_r + rW_z = 0. \tag{4}$$

Boundary conditions for the problem without vertical walls are:

$$\text{at } z = 0, \quad V = U = 0, \text{ no slip at the bottom,}$$

$$\text{at } z = H/D, \quad V_z = U_z = 0, \text{ no stress on the free surface,}$$

and

$$\int_0^{H/D} U dz = -\tfrac{1}{2}, \text{ constant radial volume flux.}$$

For $H \gg D$ the solution of the underlined equations is the Ekman solution

$$V = 1 - e^{-z}\cos z, \quad U = -e^{-z}\sin z, \quad P_r = 1.$$

It should be noted that the functions U, V, and P are independent of radius. However, the dimensional velocity components are inversely proportional to radius and are given by

$$u = -(S/\pi r' D)\,(e^{-z'/D}\sin z'/D), \quad v = (S/\pi r' D)\,(1 - e^{-z'/D}\cos z'/D).$$

In an unpublished report (Faller 1962) it has been shown that by means of a power-series expansion of the dependent variables in Ro equations (1)–(4) may be systematically reduced to the ordered equations

$$Ro^0\text{:} \quad V_{zzzz}(0) + 4V(0) = 4P_r(0),$$

$$Ro^1\text{:} \quad V_{zzzz}(1) + 4V(1) = 4P_r(1) - V_{zz}(0)^2 - 4V(0)^2,$$

$$Ro^2\text{:} \quad V_{zzzz}(2) + 4V(2) = 4P_r(2) - 2V_{zz}(0)\,V_{zz}(1) - 8V(0)\,V(1).$$

These and the higher-order equations may be derived from the equation

$$V_{zzzz} + 4V = 4P_r - Ro(V_{zz}^2 + 4V^2),$$

where use has been made of the fact that the radial derivatives of the basic equations vanish at each order as a result of the expansion in Ro. This is because the zero-order solution and the boundary conditions are independent of r. For large z the solution to second order in Ro is

$$U = 0, \quad V = 1 - \tfrac{3}{10} Ro + \tfrac{233}{600} Ro^2 + \ldots.$$

This theoretical solution will be compared with observations as one method by which the critical Reynolds number for transition from laminar flow has been determined.

Prior to discussion of the experimental data it is convenient to present the rationale for the selection of a set of non-dimensional parameters which appear to be of physical significance for the interpretation of the data. A general observation was that in each experiment the instability occurred within a critical radius r_c'. This radius should be a function of the independent parameters alone, as expressed by the relation $r_c' = f(S, \Omega, \nu, H)$. With two basic dimensions, length and time, and with five variables three non-dimensional numbers may be formulated (for example, see Bridgman 1931) and these have been selected as follows. If the instability occurs primarily in the boundary layer one should perhaps expect the onset of instability to occur at a critical value of a Reynolds number given by $Re = vD/\nu$. Using the zero-order solution for the tangential flow at large z, $v = S/\pi r' D$, we define a Reynolds number in terms of the independent parameters alone as $Re \equiv S/\pi r' \nu$. It follows that with any observed r_c' and values of S and ν there is a corresponding critical Reynolds number, $Re_c = s/\pi r_c' \nu$ below which ($r' > r_c'$) we observe laminar flow and above which ($r' < r_c'$) the flow is not laminar. Since the circulation and the character of the boundary-layer flow have been found to be functions of Ro we select Ro_c as a second non-dimensional number, where Ro_c is the Rossby number evaluated at r_c'. The third independent number must contain H and we choose Ek, the Ekman number, which is the ratio of the depth of the boundary layer to the total depth of fluid. Therefore, a relation of the form $Re_c = f'(Ro_c, Ek)$ should apply apart from uncontrolled environmental conditions and within the limits of observational accuracy Similarly, the wavelength at instability should be expressible as

$$l_c = g(S, \Omega, \nu, H).$$

The natural dimension to which l_c might be related is D, and a relation of the form

$$l_c/D = g'(Ro_c, Ek)$$

might be expected to be a useful one.

The above relations should be particularly simple and useful if the instability is primarily of a boundary-layer character. Anticipating the discussion of the observational data the results may be summarized by saying that: (1) no significant relation has been found involving Ek, and (2) after consideration of and correction for certain systematic errors l_c/D appears to be constant within experimental error, and the dependence of Re_c upon Ro_c is small.

4. The experimental data

The observed circulation

Figure 5 contains 3 profiles of the observed zonal circulation as a function of radius where the ordinate is the observed non-dimensional circulation, $C_{ob} = r'v/\Omega R^2$. Values of v were determined from $v = \theta\Omega r'/\Theta$, where θ/Θ is the ratio of the relative angular displacement of the fluid θ to the absolute displacement of the tank Θ as determined from a sequence of instantaneous photographs. Included in figure 5 are the theoretical zero-order and second-order

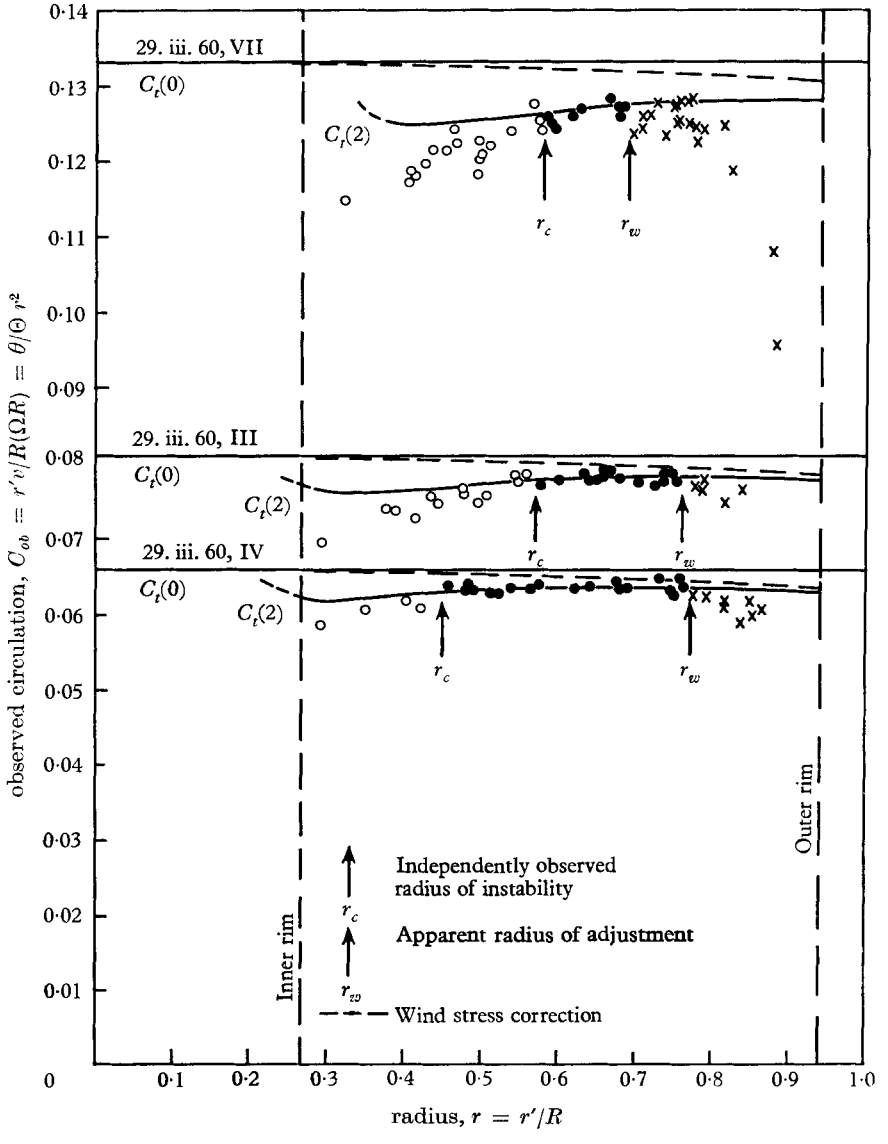

FIGURE 5. Comparison of observed circulations with theory. ×, Region of adjustment; ●, balanced laminar flow; ○, waves or turbulence.

circulations $C_i(0)$ and $C_i(2)$, and the plotted points are the observed values. Arrows r_c indicate the radii at which the instability was observed to occur by means of the dye tracer in the boundary layer.

In each case three regions of flow may be distinguished: (1) a region of lateral boundary-layer adjustment extending from the outer rim to radius r_w where departures from the theory became very small; (2) a region of balanced laminar flow which had values of circulation close to those predicted by the theory; (3) a region beginning near r_c where the circulation departed from the theory. Because the second-order solution is not reliable for large Ro, as indicated by the dashed portions of $C_i(2)$ the inference that the systematic departures from the theory are due to the instability must be supported by further analysis of the data.

Individual observations of the zonal flow from all suitable† experiments with circulation data have been combined by expressing them in terms of the non-dimensional *normalized* circulation which is defined by $V_{ob} = (\theta/\Theta)\, 1/2Ro$. V_{ob} would have the value unity if an observed value of circulation were exactly equal to the zero-order solution. Departures of the observations from the theory are defined by

$$\Delta V = V(2) + V_W - V_{ob},$$

where V_W is a small correction to the theory to account for wind stress (see Appendix). Figure 6 is a plot of all values of ΔV in the laminar regions (solid circles) and all data with $Ro < 0{\cdot}250$ from the turbulent regions (open circles). The division between laminar and turbulent data was based upon the visual observations of the critical radii. Horizontal single and double bars indicate average values of ΔV in 10 unit intervals of Re for the laminar and turbulent data respectively.

Since Re and Ro are fairly well correlated for these data a partial correlation analysis was made to determine the degree to which ΔV was independently related to Ro and Re. A significant dependence of ΔV upon Ro would suggest a failure of the second-order theory to represent correctly the basic circulation. Using the subscripts 1, 2 and 3 to represent ΔV, Re and Ro, respectively, the correlation coefficients were found to be

$$r_{12} = +0{\cdot}627,\ r_{13} = +0{\cdot}321,\ r_{23} = +0{\cdot}505;\ r_{12.3} = +0{\cdot}569,\ r_{13.2} = +0{\cdot}001,$$

where the third subscripts in the latter two (partial) correlations represent those variables which were held effectively constant by the partial correlation method (for example, see Hoel 1947). The last figure, which denotes the correlation of ΔV with Ro while Re was held effectively constant, clearly indicates that the systematic departure of ΔV from 0 was related independently only to Re. The lack of a significant partial correlation with Ro supports the theory as a valid representation of the basic unperturbed circulation. The line of linear regression of ΔV upon Re is given by

$$\Delta V - 0{\cdot}0224 = 0{\cdot}606 \times 10^{-3}(Re - 173), \tag{5}$$

† In some experiments the region of adjustment near the rim extended too far inward and overlapped the turbulent region to the extent that one could not be certain of the significance of the observed circulation.

and the intersection of this line with $\Delta V = 0$ gives a first estimate of the critical Reynolds number, $Re_c = 136$.

Because the circulation data was classified into laminar and turbulent sets on the basis of the visual estimates of r_c from the bands of dye, the intersection $Re_c = 136$ is not entirely independent of the visual observations. This possible bias was eliminated in a computation with omission of data in the range $150 > Re > 120$. The slope in (5) was changed to $0{\cdot}528 \times 10^{-3}$ and the intersection of the lines in the laminar and turbulent regions gave the estimate $Re_c = 126$.

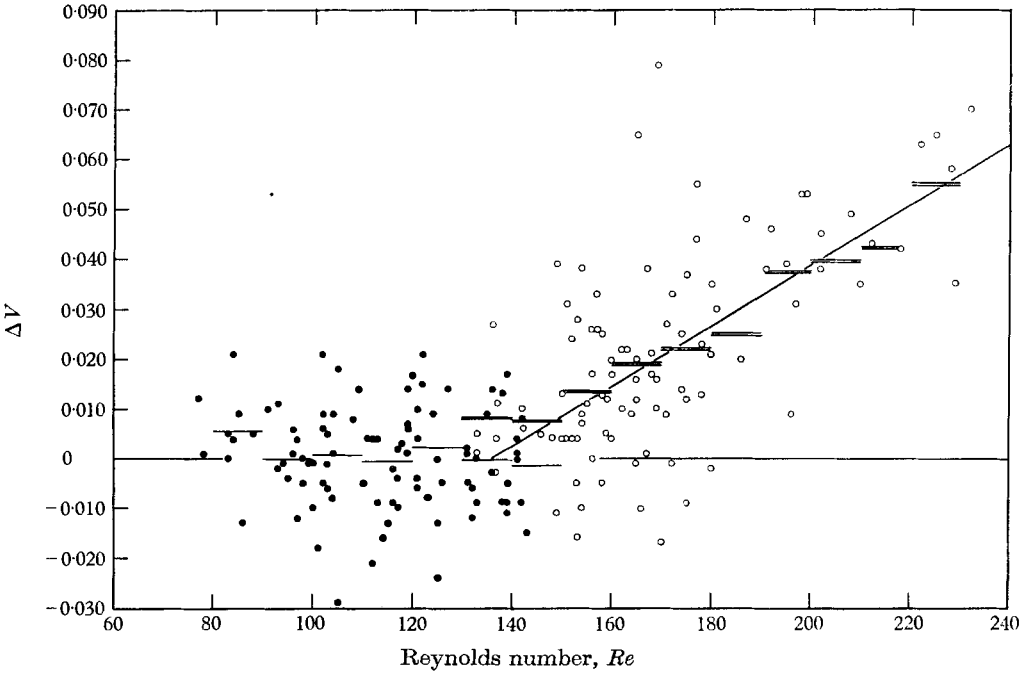

FIGURE 6. Departures of the normalized observed circulation from the second-order theory as a function of Reynolds number. Horizontal single and double bars indicate average values of ΔV for ten-unit intervals of Re in the laminar and turbulent regions, respectively. ● Laminar flow; ○, waves or turbulence.

The difference between these two values is some measure of the uncertainty in the value of Re_c computed from the circulation data. The scatter of points from a constant value in the laminar region and from the regression line in the turbulent region may appear to be large in figure 6. However, the standard deviation of ΔV in the laminar region is only 1·0 % of the total circulation. This spread is readily explicable in terms of errors of observation of the angle θ which was independently estimated to have errors with a standard deviation of approximately 1 %. In the turbulent region the correlation explains 39 % of the variance of ΔV leaving an unexplained spread from the regression line with a standard deviation of 0·016, or 1·6 % of $V(2)$. These considerations indicate that in the absence of observational errors the correlation between ΔV and Re for this range of Re could be expected to approach unity.

From the three examples of figure 5 it may be seen that the width of the boundary zone of adjustment near the outer rim increases with circulation and is significantly wider than would be estimated by laminar boundary-layer theory. Estimates from a boundary-layer analysis indicate vertical boundary-layer widths of approximately 1 to 2 cm. But with such narrow boundary layers at the outer rim the critical value for centrifugal instability would be far exceeded. The observed wide zones of adjustment near the outer rim are believed to be primarily a consequence of centrifugal instability for two reasons: (1) the observed

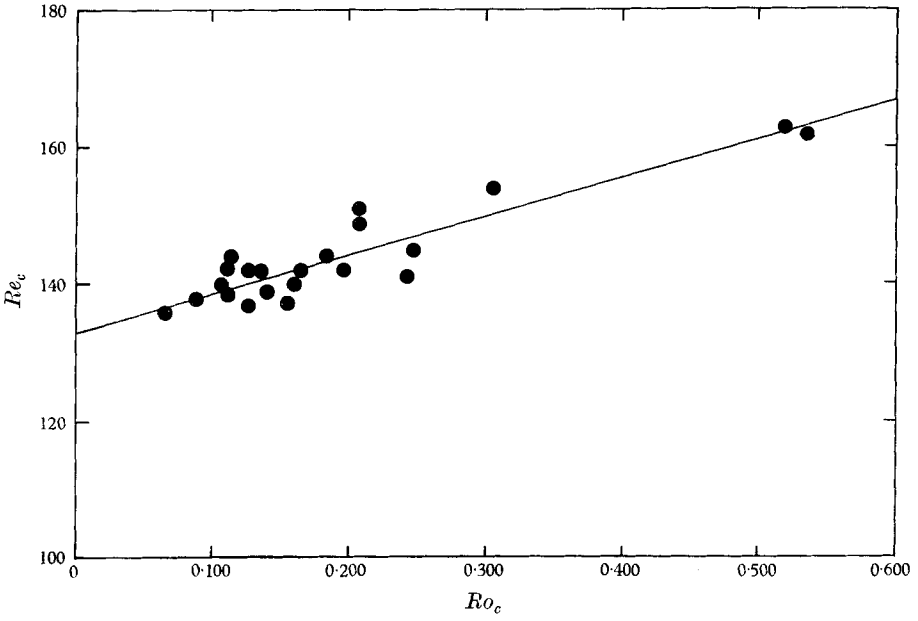

FIGURE 7. Dependence of the critical Reynolds number upon Rossby number at the observed critical radius.

shears were close to the values required for stability; and (2) near the inner rim at $r = 0{\cdot}27$ (where the shear was in the centrifugally stable sense) the widths of the vertical boundary layers were observed to be of the order of 1 to 2 cm, in agreement with laminar boundary-layer theory.

The observed instability

Observations of the average radius at which the bands of dye appeared to originate are recorded for each experiment in table 1 as r_c, the critical radius. In cases where r_c appeared to vary with longitude the maximum radius at which the bands were clearly observable was selected, and the estimated standard deviation of error in r_c is 0·01. In figure 7, Re_c is plotted as a function of Ro_c where each of these numbers is computed at r_c. Experiments in which the instability occurred within the boundary zone of adjustment near the rim have been omitted. The reported data are based upon the analysis of photographs of which the illumination, film exposure and development were constant, so that the photographic data are considered to form a reasonably homogeneous set. The linear correlation

of Re_c with Ro_c is 0·90 leaving an unexplained variance in Re_c of 19%. Thus the scatter of points from a straight line in figure 7 is largely explicable in terms of errors of observation of r_c, since a standard deviation of error in r_c of 0·01 would explain 12 % of the variance of Re_c.

Extrapolation of the linear regression line to $Ro_c = 0$ (zero curvature) gives the estimate $Re_c = 133$ for linear Ekman flow. Systematic observational errors associated with the necessity of finite amplitude waves for the detection of the

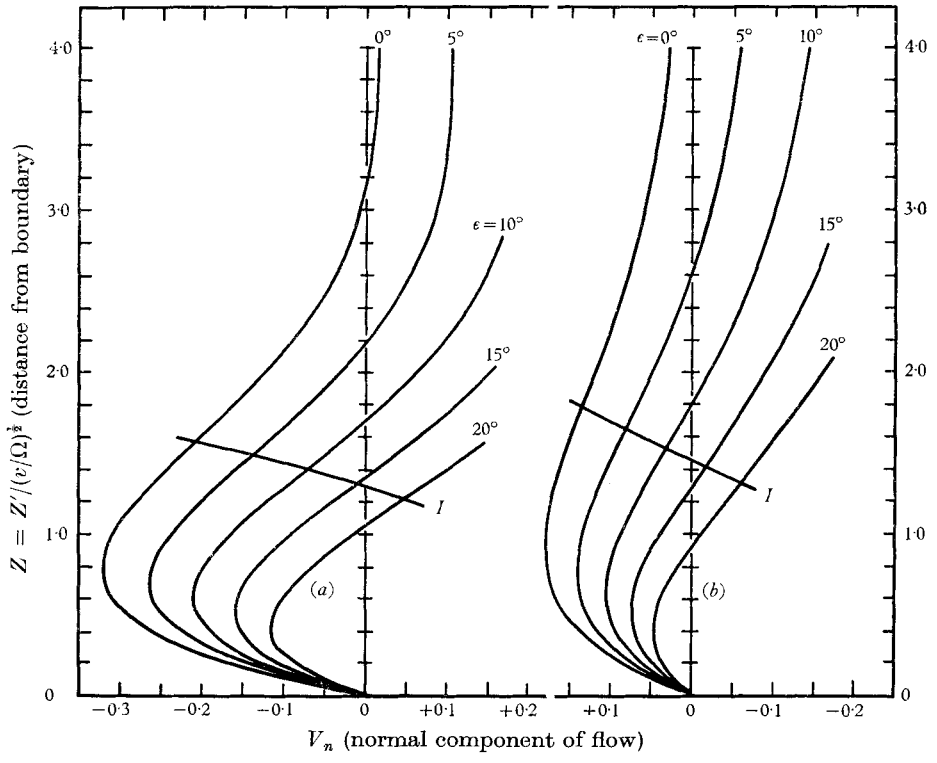

FIGURE 8. Boundary-layer components normal to the direction at angle ϵ with the tangential direction. (*a*) Ekman boundary-layer profiles ($Ro = 0$). (*b*) Rotating-disk boundary-layer profiles.

instability have been considered in detail in an unpublished report (Faller 1962). By means of an assumed model of the character of the perturbations, and consideration of the minimum amplitude perturbation detectable with the dye, it has been determined that Re_c at $Ro_c = 0$ is overestimated by approximately 9 ± 5. This correction reduces the value of Re_c at $Ro_c = 0$ to 124 ± 5. Furthermore, it is probable that the *slope* of the regression line in figure 7 should be reduced somewhat, but the magnitude of this latter correction is quite uncertain.

Considering the two independent estimates of Re_c, from the circulation data and from the direct observations of r_c, it would appear that the true value lies in the range $120 < Re_c < 130$. It is difficult to assess the relative merits of the two methods and each has an uncertainty of approximately ± 5. Therefore, the value $Re_c = 125 \pm 5$ is taken as the most reasonable estimate from the

available data of the critical Reynolds number for the laminar Ekman boundary layer.

Some mention should be made of the frequent occurrence of other types of banded structure which, when present, usually obscured the bands which have been described. These were characterized by a larger spacing and by a zero angle with respect to the zonal direction or by an angle opposite to that of the smaller bands. These bands are well represented in figure 4 (plate 4*d*) where they all but obscure the smaller waves, and they may also be seen in figure 4 (plate 3*a*) between the radii 6 and 7. Frequently they seemed to grow out of the smaller bands and at times they occurred at a radius greater than was expected for instability, sometimes extending to the rim. But in any given experiment it was difficult to assign a specific radius of formation and they appeared to have no relation to the non-dimensional parameters of the problem. It is felt that in most cases these larger banded forms were related to mechanical disturbances or to irregular boundary conditions, but the possibility of another form of instability of the laminar flow cannot be discounted.

Band spacings and angles

On the one hand, one might expect that the angles of the bands would be independent of radius and, therefore, that the bands would spiral inward as equiangular spirals. On the other hand, one might reason that the band spacing should remain constant and proportional to D. It has been found from photographs that in some cases the spacing did at first decrease with decreasing radius (following the equiangular hypothesis) but at smaller radii the waves began to readjust by folding into one another with a reduction of angle thus maintaining an approximately constant spacing (see figure 4, plate 3*a*).

The observed average spacing for each experiment $\bar{l}_c$, measured as close to r_c as was possible, and the average angle $\bar{\alpha}$ with respect to the tangential direction are presented in table 1. Because of the proportional dependence of l_c upon radius for equiangular spirals the non-dimensional values were adjusted by the factor $r_c/\bar{r}$ to give $L = (\bar{l}_c/D)(r_c/\bar{r})$ where $\bar{r}$ is the mean radius at which the spacings were measured. Thus L represents an estimate of the non-dimensional wavelength corrected to the observed critical radius. These values L show no significant dependence upon Ro_c or upon Ek and have an average for all experiments of $L = 10{\cdot}9$. The frequency distribution of observation of angle α for 188 observations from 23 experiments gave the average angle $\bar{\bar{\alpha}} = 14{\cdot}5$ degrees with the standard deviation $\sigma_\alpha = 2{\cdot}0$ degrees. This distribution may be non-representative because some subjectivity was necessary for the selection of bands sufficiently well formed to measure. The average angles for each experiment (table 1) show real differences from one experiment to another and have a linear correlation with Ro_c of $+0{\cdot}52$, but again systematic errors of observation cannot be discounted as a possible source of the apparent relationship.

Band motions

Motion pictures of the bands clearly show that in all cases observed the bands had a component of motion normal to their axes, radially inward. Before

presentation of the analysis of the band motions it is necessary to discuss briefly some of the results of Stuart's theoretical analysis (GSW) of the instability of the flow over a rotating disk. Stuart demonstrated theoretically the possible existence of unstable modes at infinite Reynolds number in the form of roll vortices. In particular he discussed a class of modes stationary with respect to the rotating disk, inasmuch as stationary streaks were directly observed on the disk by the

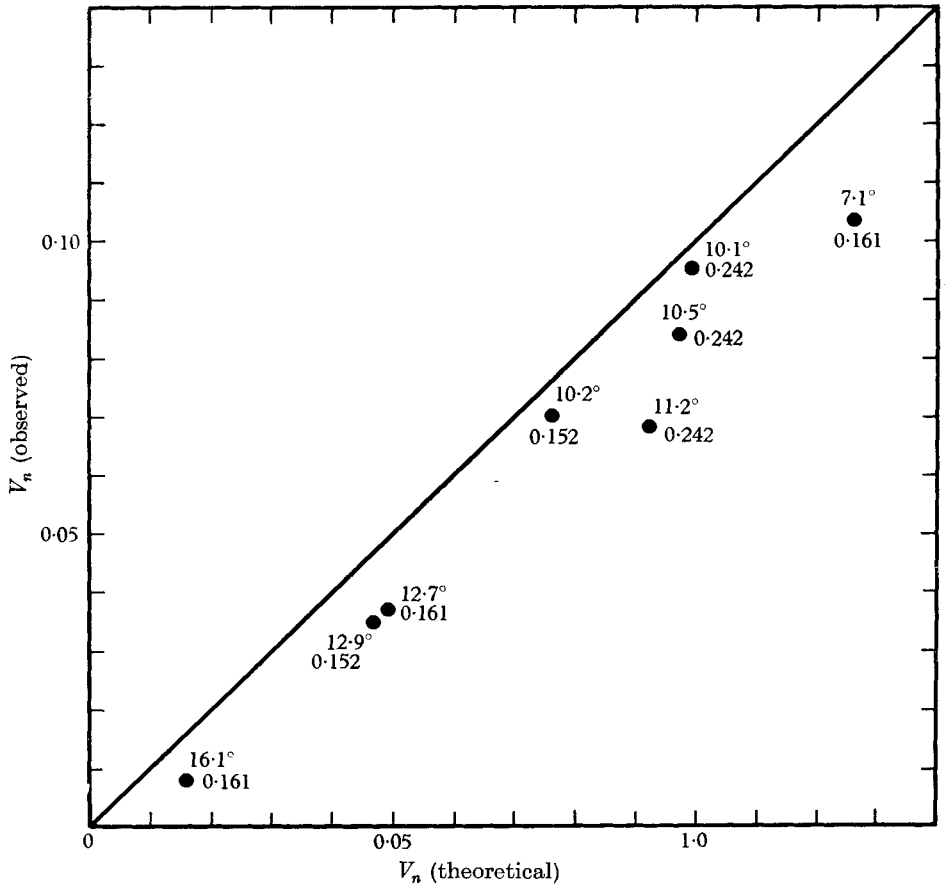

FIGURE 9. Observed speeds of bands (normal to their axes) compared with theoretical normal speeds. The V_n (theoretical) are based upon observed angles (upper figures) and boundary-layer profiles for the specified values of Ro (lower figures).

china-clay technique. From Stuart's theory the orientation of a stationary mode was deduced to be along that direction for which the profile of the normal component of the boundary-layer flow V_n *vs* height had an inflexion point coincident in height with a zero value of the normal flow. A physical interpretation of this criterion is that the instability is associated with the inflexion point of such a profile, and that if a perturbation of infinitesimal amplitude exists and is stationary its angle must be such that there is no advective normal component of flow at the level of the centre of the vortex tube. Figure 8 illustrates the graphical determination of that angle for the two boundary layers under discussion.

Corresponding to any angle ϵ one plots the normal component of flow *vs* height, and for each ϵ there exists a first inflexion point I. The angle for which this inflexion point coincides with $V_n = 0$ is 13·3 degrees for the rotating disk flow and 16·0 degrees for the Ekman spiral. It is noteworthy that the observed stationary angle on the rotating disk was approximately 14 degrees which fact tends to confirm Stuart's theory.

By extension of the above argument concerning the angle required for stationary modes we may hypothesize that bands formed at some other angle and at the inflexion point associated with that angle should have an advective normal component of motion. For example, from the Ekman profiles of figure 8 bands with an angle of 5 degrees would have the 'theoretical' normal speed $V_n = -0{\cdot}14$ at the height of the inflexion point I. Band angles and the corresponding speeds of motion were evaluated for some 8 cases for which motion pictures were available, and the observed normal speeds *vs* the theoretical speeds are presented in figure 9. For determination of the theoretical values the slightly different second-order boundary-layer profiles corresponding to the observed values of *Ro* were used in place of the curves of figure 8. Numbers beside each observation point of figure 9 indicate the observed average angles and the Rossby numbers at the average radii of observation of each group of bands. The agreement between observed and predicted speeds tends to support the general argument that the instability is associated with the inflexion point of the component of flow normal to the bands.

5. Concluding remarks

These studies have established a critical Reynolds number for the instability of the laminar Ekman boundary layer and several characteristics of the unstable waves, including their wavelengths, angles, speeds of propagation, and the effect of the boundary-layer instability upon the basic tangential circulation. Some of the results are based upon limited data and therefore require corroboration by further experimental studies. Unfortunately, because of damage from high water, salt, seaweed, and sand as a result of a hurricane in the fall of 1960 the apparatus was unsuitable for further experimental work and has been dismantled. Consequently, there is no possibility of obtaining further data with the same apparatus. To obtain unstable flow at low Rossby numbers, as was the primary goal of this study, comparably large experimental apparatus or a much higher rotation rate is required, as may be deduced from the definitions of *Re* and *Ro*.

Some interesting differences from corresponding data of the rotating disk experiments should be emphasized. The value $Re_c = 125 \pm 5$ for the Ekman flow is substantially different from the corresponding value defined in the same way for the rotating disk, namely $Re_c = 436$. Without an adequate theory to explain either value one may speculate on the significance of obvious differences in the two boundary-layer profiles, the most conspicuous difference being the stronger radial component in the Ekman flow (see figure 8 for $\epsilon = 0$ deg.). The ratio of vertical shears of the normal components of flow at the inflexion points

corresponding to the stationary angles for the two cases is approximately 2·2, and this difference in shears is perhaps the major contribution to the large ratio of observed critical Reynolds numbers. Furthermore, in the rotating disk case there is a normal flow into the boundary layer (due to the net lateral divergence in the boundary layer) which may tend to stabilize the flow.

The spacing of the streaks on the rotating disk has been found from the data of GSW to be $21{\cdot}5D$ compared to $5{\cdot}5D$ predicted by Stuart's analysis and compared to $10{\cdot}9D$ found here for the Ekman instability. Stuart tentatively ascribed the factor of 4 difference to the omission of viscosity in the instability theory, but it is noteworthy that the value found for the Ekman flow is very close to the integral factor 2 times Stuart's theoretical value. This apparent quantization may be incidental or may represent a tendency for the viscous coupling between the boundary and the perturbation to produce subharmonics of the preferred inviscid mode.

Sincere appreciation is extended to Mr Delvin Stern who took part in the early phases of the observational programme and to Dr George Veronis who together with Dr Stern has offered valuable suggestions for the preparation of the initial manuscript.

The research reported in this paper was supported in part by Contract Nonr-2196(00) with the Office of Naval Research and in part by Contract AF 19(604)-4982 with the Geophysics Research Directorate.

Appendix

Because of the basic rotation of the tank with respect to the air at rest in the laboratory there is a stress on the free surface of the water which may be determined in theory from the classical analysis of the flow over a rotating disk (for example, see Schlichting 1960). It may be shown that for slow flow within the rotating tank the tangential wind stress on the water is equal at each radius to the stress of the wind-induced flow on the tank. This balance leads directly to the equation for the wind induced flow

$$v_W = (\rho_a/\rho_w)\,(\nu_a/\nu_w)^{\frac{1}{2}}\,\Omega r G'(0),$$

where subscripts a and w refer to the physical properties of air and water, v_W is the resultant wind-induced zonal flow, and $G'(0) = -0{\cdot}616$ is the non-dimensional vertical shear of the tangential component of the air flow evaluated at the surface of a rotating disk. The non-dimensional wind-induced circulation as a function of r is $C_W(r) = C_W(R)\,r^2$, where $C_W(R) = 0{\cdot}0027$ is virtually constant for all experiments. This result has been confirmed experimentally, and the dashed lines in figure 5 indicate the amount subtracted from the zero-order circulations to account for the wind stress. The corresponding *normalized* wind-induced circulation is given by

$$V_W = C_W(R)/2Ro.$$

REFERENCES

ARONS, A. B., INGERSOLL, A. P. & GREEN, T. 1961 Experimentally observed instability of a laminar Ekman flow in a rotating basin. *Tellus*, **13**, 31–9.

ARX, W. S. VON 1955 An experimental study of the dependence of the primary ocean circulation on the mean zonal wind field. Doctoral dissertation, M.I.T.

BRIDGMAN, P. W. 1931 *Dimensional Analysis*, 2nd ed. New Haven: Yale University Press.

COCHRAN, W. G. 1934 The flow due to a rotating disc. *Proc. Camb. Phil. Soc.* **30**, 365.

DORSEY, N. E. 1940 Properties of ordinary water substance. *Amer. Chem. Soc. Mono.* no. 81. New York: Rheinhold Publ. Co.

EKMAN, V. W. 1905 On the influence of the earth's rotation on ocean currents. *Ark. Mat. Astr. Fys.* **2**, no. 11.

FALLER, A. J. 1960 Further examples of stationary planetary flow patterns in bounded basins. *Tellus*, **12**, 159–71.

FALLER, A. J. 1962 The development of fluid model analogues of atmospheric circulations. *W.H.O.I., Final Rep.* Contract AF 19 (604)-4982, GRD, AFCRL.

FETTIS, H. E. 1955 On the integration of a class of differential equations occurring in boundary layer and other hydrodynamic problems. *Proc. 4th Midwest Conf. Fluid Mech.*

GREGORY, N., STUART, J. T. & WALKER, W. S. 1955 On the stability of three-dimensional boundary layers with application to the flow due to a rotating disk. *Phil. Trans.* A, **248**, 155–99.

GREGORY, N. & WALKER, W. S. 1960 Experiments on the effect of suction on the flow due to a rotating disc. *J. Fluid Mech.* **9**, 225–34.

HAURWITZ, B. 1935 On the change of wind with elevation under the influence of viscosity in curved air currents. *Gerland's Beitrage zur Geophysik*, **45**, 243–67.

HOEL, P. G. 1947 *Introduction to Mathematical Statistics.* London: Chapman and Hall.

HOWARD, L. N. 1961 A note on the existence of certain viscous flows. *J. Math. Phys.* **40**, 172–6.

KÁRMÁN, TH. VON 1921 Laminare und turbulente Reibung. *Z. angew. Math. Mech.* **1**, 233–52.

LIN, C. C. 1955 *The Theory of Hydrodynamic Stability.* Cambridge University Press.

ROGERS, M. H. & LANCE, G. N. 1960 The rotationally symmetric flow of a viscous fluid in the presence of an infinite rotating disc. *J. Fluid Mech.* **7**, 617–31.

SCHLICHTING, H. 1960 *Boundary Layer Theory*, 4th ed. New York: McGraw-Hill.

STERN, M. E. 1960 Instability of Ekman flow at large Taylor number. *Tellus*, **12**, 399–417.

STEWARTSON, K. 1953 On the flow between two rotating co-axial discs. *Proc. Camb. Phil. Soc.* **49**, 333.

STUART, J. T. 1954 On the effects of uniform suction on the steady flow due to a rotating disc. *Quart. J. Mech. Appl. Math.* **7**, 446–57.